RSC Advances

ROYAL SOCIETY OF CHEMISTRY

www.rsc.org/advances

RSC Advances

ARTICLE

Biomass derived xylose Guerbet surfactants: thermotropic and lyotropic properties from small-angle X-ray scattering

Received 00th January 20xx,
Accepted 00th January 20xx

DOI: 10.1039/x0xx00000x

www.rsc.org/

Chia Yen Liew, Malinda Salim, N. Idayu Zahid and Rauzah Hashim*

A series of novel branched-chain glycosides were synthesise from xylose, an aldopentose and Guerbet alcohols whose total number of carbon atoms ranges from C_8-C_{24} . The thermotropic and lyotropic phases of the highly pure Guerbet xylosides were investigated, using differential scanning calorimetry, optical polarising microscopy and small-angle X-ray scattering. In dry condition, the shortest compound (total C_8) exhibits a monotropic lamellar (L_α) phase while the C_{12} compound forms rectangular columnar (Col_r) phase at the room temperature, a rarely reported phase in lipidic systems. The longer ones (C_{16}, C_{20} and C_{24}) adopt inverse hexagonal (H_{II}) phases. Upon hydration, the L_α phase of C_8 compound remains, and while that of the C_{12} compound exhibits an inverse bicontinuous cubic phase of space group *Ia3d* in excess water. The C_{16} and C_{20} compounds remain in the H_{II} phase upon hydrating, but the lattice parameters for the hydrated forms increase considerably. An inverse micellar *Fd3m* cubic phase is observed in the fully hydrated C_{24} compound. The amphiphilic nature of these compounds coupled with the ability to form inverse non-lamellar phases at the room temperature makes them ideal candidates for a variety of applications such as controlled release drug-carrier.

1. Introduction

D-xylose is a major constituent of a pentose fraction in hemicellulose, a plant cell wall heteropolysaccharide derived from the renewable lignocellulosic biomass. This monosaccharide differs from glucose such that a proton replaces the hydroxymethyl $-CH_2-OH$ group at the carbon number five, thus making it a five carbon sugar ring. As xylose is abundant in nature (up to 40% lignocellulosic biomass is hemicellulose), extensive work has been done to convert xylose into useful products and low-cost energy source. One most noticeable application is in the production of xylitol, a low-caloric sweetener and an anti-cavity agent in dental products.[1] In addition, the alkyl xylosides have been proved for their effectiveness as wetting agent for paper impregnation in the wood production.[2] The synthesis and systematic study of thermotropic liquid crystals phase of the monoalkylated β-D-xyloside has been done by Xu *et al*.[3] All the compounds exhibit mesomorphic properties and they have also found that monoalkyl xylosides have low toxicity towards human cells, which suggests their potential usefulness as cosmetic and detergent products. Recently, a direct preparation of monoalkyl xylosides and oligoxylosides from xylan in aqueous medium using xylanases has been proposed.[4] This enzymatic synthesis route occurs in mild conditions and converts the lignocellulosic biomass into useful green sugar surfactants.

A sugar base surfactant, xyloside, belongs to the larger chemical family of glycolipid, which can be found naturally or synthesised. The natural ones are normally found on the exterior of cell surface membranes, and they play vital roles in cell processes like cell-cell recognition and cell membrane structural stabilisation.[5, 6] Most glycolipids in biomembranes are double-chained (saturated and/or unsaturated) with 16 to 18 carbons per chain.[7, 8] Highly pure natural glycolipids are difficult to extract, and their total synthesis often proves challenging,[9, 10] which makes synthetic substitutes become increasingly in demand. One of these is the di-alkylated or branched-chain glycolipid which is isostearic to many natural lipids. Hence it has the propensity to mimic the property and function of natural lipids.

Lyotropic liquid crystal self-assembly is governed by local constraints, and the type of phase formed can be estimated using the critical packing parameter (CPP) proposed by Jacob Israelachvili,[11] which is defined as $v/a_0 l_c$ where v is the volume of the hydrophobic chain, a_0 is the interfacial area occupied by the hydrophilic head group, and l_c is the length of the hydrocarbon chain. According to the theory, when the CPP is equal to one, lamellar phase will be observed. On the other hand, a CPP less than one will give a normal phase and when it is greater than one, an inverse phase is formed. In general, the double alkyl chain in glycolipid increases the chain bulkiness v/l_c and thus increases the CPP. [12, 13] Moreover, several authors have reported the formation of inverse phases by

Center of Fundamental Science of Self-Assembly, Department of Chemistry, Faculty of Science, University of Malaya, 50603, Kuala Lumpur, Malaysia. E-mail: rauzah@um.edu.my

† Footnotes relating to the title and/or authors should appear here.
Electronic Supplementary Information (ESI) available: [details of any supplementary information available should be included here]. See DOI: 10.1039/x0xx00000x

double alkyl chains glycolipids.[14-17] More specifically, the observation of a stable hexagonal phase in coexistence with excess water is itself a strong evidence of the formation of an inverse phase. [18] Thus, the branched-chain Guerbet xylosides are more likely to adopt non-lamellar phases compared to their monoalkylated counterparts.[14-16, 19]

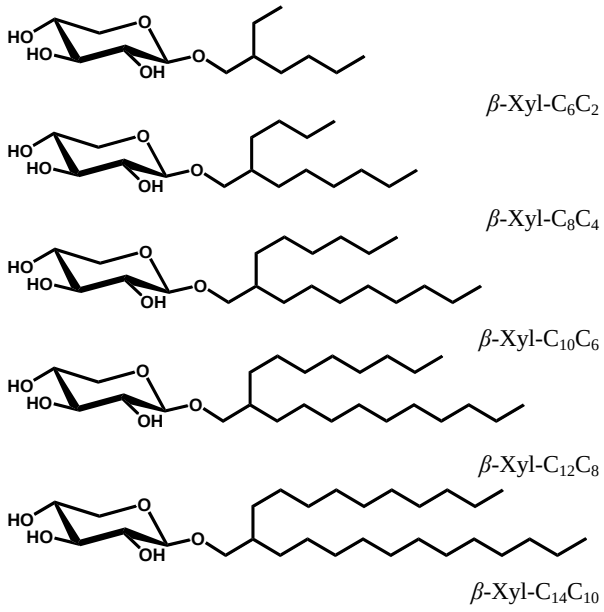

Fig. 1 The chemical structures of the branched-chain β-D-xylosides studied. The degree of chain branching [20] ranges from 0.75–0.58.

Numerous applications such as drug delivery system[21] and membrane protein crystallisation have been attempted using these branched glycolipids.[22]

A relatively new branched-chain design has been proposed using Guerbet alcohols. The branched alkylated hydrophobic tail contains two asymmetric chains ranging from C_6C_2, C_8C_4, $C_{10}C_6$, $C_{12}C_8$ to $C_{14}C_{10}$. This shortest and longest branched chain design has a degree of branching [20] of 0.75 and 0.58 respectively, while for the monoalkylated chain this factor equals to 1. Different selection of mono- and disaccharide sugars head groups with Guerbet branched-chain has been synthesised, and the effect of stereochemistry on the liquid crystal properties were investigated.[17, 19, 23] The phase boundaries exhibited by these systems tend to be relatively insensitive to temperature. As expected from previous experimental results, [17, 19] stable inverse non-lamellar phases in excess water condition have been observed for these compounds. In an ensuing study, a xylose (an aldopentose) sugar head group is used to prepare the Guerbet surfactants in order to exploit an abundant biomass natural product for surfactant applications and expand systematically the stereochemistry investigation of these sugar lipids. Their chemical structures are depicted in Fig. 1. The phases are designated using the standard lyotropic nomenclature in both dry and fully hydrated states because the molecules involved are amphiphilic rather than mesogenic.[19]

2. Experimental section

2.1 Guerbet xyloside synthesis

The starting xylose sugar, D-(+)-Xylose (99%) and five Guerbet branched-chain alcohol (97%), of total chain length C_8, C_{12}, C_{16}, C_{20} and C_{24} were purchased from Sigma-Aldrich. Boron trifluoride diethyl etherate and ACS grade solvents including acetonitrile, 1-butanol, dichloromethane, ethyl acetate, ethanol, and n-hexane were supplied from Merck. All chemicals and solvents were used without any further purification. The Guerbet xylosides were synthesised following a reported procedure,[23] and their anomeric purity was estimated to be ≥ 97% according to ^{1}H NMR, ^{13}C NMR, HPLC and thin layer chromatography. All the glycolipids were extensively lyophilised before characterisation by keeping the lipids in a vacuum oven over di-phosphorous pentoxide for at least 48 hours. The lyophilised forms of these xylosides are refereed as dry or anhydrous lipids in the present work. The term "dry" is used rather loosely because it is a well-known fact that removing the last trace of water is difficult in sugar lipids. [24] Thus, we have tested these consistently "dry lipids" using a Fourier Transform Infrared Spectroscopy (FTIR) for the assessment of their water content by observing the stretching and bending modes. We had used the lipids that have been lyophilised (dry), lipids that are left at room temperature for 96 hours (ambient hydrated), and lipids in excess water. The typical FTIR spectra of these three samples (from β–Xyl-C_8C_4) are shown in the Supporting Information (Fig. S1). The result shows that in the stretching region (ca. 3600-3200 cm^{-1}), the IR peak from the dry sample is smaller compared to the other two. It should be noted that the broad peak in this region also indicates presence of the contributing stretching vibration of the -OH group of the lipid. On the other hand, the water bending mode (ca. 1700-1600 cm^{-1}) is almost negligible for the lyophilised (dry) lipid compared to the other two systems, implying that our assumption of the "dry lipid" is not unreasonable. NMR data for a homologous series of xylosides are available in the Supporting Information.

2.2 Differential scanning calorimetry

Phase transition temperature was identified with a DSC 822^e, Mettler Toledo calorimeter equipped with Haake EK90/MT intercooler. The calorimeter was calibrated using standard Indium for temperature and enthalpy accuracy before experiments. All the samples tested were dried in a vacuum oven over di-phosphorous pentoxide for at least 48 hours. The measurements were performed at a scanning rate of 5°C/min from -40°C to 150°C after the materials were being encapsulated in the aluminium pans. The data were analysed using STAR^e Thermal Analysis System software.

2.3 Optical polarising microscopy

The liquid crystalline behaviour of xylosides was initially characterised by OPM using two microscope systems: (i) an Olympus BX51 polarising microscope equipped with a Mettler Toledo FP82HT Hot Stage and a temperature controller (FP90

Central Processor) linked to a camera (Olympus DP26); (ii) Nikon Eclipse LV100POL polarising microscope equipped with a Linkam heating stage and linked to a QImaging MircoPublisher 5.0 RTV digital camera. The captured images of phase texture are in the presence of cross-polarising lenses, with magnification factors of 10 and 20. All xylosides were consistently dried before the experiments in a vacuum oven over di-phosphorous pentoxide for at least 48 hours.

For the thermotropic studies, dry sample was transferred onto a clean glass microscope slide and covered with a thin glass cover slip. The sample was placed on the hot stage and heated until it reached its isotropic phase. The liquid crystal image that formed was taken upon slow cooling at a rate of 1°C/min to obtain the best optical textures.

For the lyotropic studies, water contact penetration experiment was used to identify the texture of the liquid crystal phase. A neat surface of sample was prepared by melting the dry sample sandwiched in between a clean microscope slide and cover slip. The sample was heated to an isotropic phase and cooled to the room temperature. A drop of deionised water was added to the edge of the glass cover slip and allowed to contact with the dry lipid by capillary force to form a concentration gradient that ranged from pure water to neat surfactant.

2.4 Small-angle X-ray scattering sample preparation

The dry samples were kept in a vacuum desiccator until the day of measurement. Excess water samples were prepared at 90% (w/w) water concentration by adding water and dry lipid into a 1.5-ml microcentrifuge tube. An exception was given to the β-Xyl-C_6C_2 where full hydration was achieved at 50% (w/w) water content. Homogenisation hydration was achieved by repeated centrifugation. The homogenised sample was equilibrated for at least three days before SAXS measurements were made. Approximately 50 mg of sample was transferred to a paste cell holder and loaded into the X-ray machine.

2.5 Small-angle X-ray scattering measurement

Scattering pattern of the dry and fully hydrated samples was characterised using an analytical small-angle X-ray scattering from SAXSess, Anton Paar Austria. The system was equipped with an X-ray tube (DX-Cu 12x0.45, SERFERT) generating Cu-K_α radiation at wavelength λ = 1.542 Å at 40 kV and 50 mA. All measurements were performed using line collimation under vacuum, and the scattering pattern was collected using a 1-D diode detector. Silver behenate (λ =58.4 Å) was used as a calibrant for all measurements. The sample temperature was controlled using a TCS 150 within an accuracy of ±0.1°C. The dry samples were heated to the isotropic phase followed by cooling to the room temperature, and were left overnight for equilibration. The final SAXS measurement was performed at 25°C. The excess water samples that have reached thermodynamic equilibrium were characterised immediately after loading. Exposure time for both types of samples was 1 h. The data was analysed using SAXSquant software package, and the liquid crystal phases were assigned using SGI software (Anton Paar, Austria) except for the rectangular columnar phase.

3. Results and discussion

3.1 Differential scanning calorimetry

Transition temperatures of the samples were obtained from the peak maxima of the second heating cycle to remove the thermal history, whereas the enthalpies were determined by integrating the transition peaks as shown in Fig. S2 of the Supporting Information.

Table 1 Thermotropic phase transition temperatures and enthalpies for the dry β-D xylosides estimated by DSC. Error in temperature is ±0.1°C while error in enthalpy is ±0.01 kJ/mol

Lipid	Melting transition temperature (°C) [enthalpy (kJ/mol)]	Clearing transition temperature (°C) [enthalpy (kJ/mol)]
β-Xyl-C_6C_2	?	53°C [8.65]
β-Xyl-C_8C_4	?	43°C [6.62]
β-Xyl-$C_{10}C_6$	?	50°C [0.50]
β-Xyl-$C_{12}C_8$	15°C [3.80]	63°C [0.83]
β-Xyl-$C_{14}C_{10}$	16°C [5.58]	56°C [0.95]

Upon heating, β-Xyl-C_6C_2 changed from its liquid crystalline phase to an isotropic phase at 53°C with ΔH = 8.65 kJ/mol. The DSC thermogram of β-Xyl-C_8C_4 gave a phase transition from liquid crystalline phase to the isotropic liquid at 43°C (ΔH = 6.62 kJ/mol). Meanwhile, a clearing temperature at 50°C with ΔH = 0.50 kJ/mol was observed for β-Xyl-$C_{10}C_6$. No other phase transitions were detected on subsequent heating and cooling for C_6C_2, C_8C_4 and $C_{10}C_6$ compounds. This implies the solid to liquid crystal phase transition occurred at a much lower temperature beyond the range of the lowest experimental temperature (-40 °C). On the other hand, β-Xyl-$C_{12}C_8$ exhibits a melting transition from the crystal phase at 15°C, and the associated enthalpy change was 3.80 kJ/mol. The enthalpy value for this transition was significantly larger than that of a liquid crystalline to isotropic state transition, indicating that β-Xyl-$C_{12}C_8$ had undergone a transition directly from a highly ordered crystalline phase to the less ordered liquid crystalline phase followed by a transition into isotropic state at 63°C with ΔH = 0.83 kJ/mol. Similarly, β-Xyl-$C_{14}C_{10}$ melted at 16°C with ΔH = 5.58 kJ/mol from the crystal phase. At 56°C, β-Xyl-$C_{14}C_{10}$ changed from liquid crystalline state to the isotropic liquid state with ΔH = 0.95 kJ/mol. All the DSC data is tabulated in Table 1.

Glycosides usually behave like a common liquid crystal mesogen which melts from the crystal phase through a liquid crystal phase into the isotropic liquid. In addition, from the DSC results, these Guerbet xylosides melt at sub-ambient temperatures implying they are liquid crystalline at room temperature. Usually for monoalkylated glycolipids, the clearing temperature increases with increasing alkyl chain length.[3] However, due to the Guerbet chain branching, such trend was not apparent for β-D-xylosides series as has been

the case for other Guerbet glycolipids with glucose and galactose head groups.[19, 23]

3.2 Optical polarising microscopy

The thermotropic and lyotropic liquid crystalline phase of xylosides were further identified by optical polarising microscopy (OPM). Generally, when observed under crossed polarisers, both cubic and micellar phases were optically isotropic and black but they are distinguishable from each other because the former, when pressed, was more viscous than the latter. On the other hand, the lamellar and hexagonal phases give distinctly different birefringent textures, where the latter gives much larger domains compared to the former.

On heating, dry β-Xyl-C_6C_2 started to melt at 48°C and became completely isotropic at 53°C. When the sample was cooled, a focal-conic fan-shaped texture appeared at 19°C, suggesting a lamellar (L_α) phase (Fig. 2a). Upon addition of water to the neat surface of dry β-Xyl-C_6C_2, myelin figures formed slowly and grew into elongated tubes at the edge of the bulk sample as shown in Fig. 2b. The observation confirmed the presence of an L_α phase in the dry and hydrated samples.

Neat β-Xyl-C_8C_4 also gave focal-conic texture with stronger birefringence compared to that of β-Xyl-C_6C_2 under OPM (Fig. 2c). Upon heating, the birefringence texture became clear at 43°C and the focal-conic texture reformed at 25°C upon cooling. The highly birefringent texture suggested an inversed hexagonal phase (H_{II}) prevails in dry β-Xyl-C_8C_4. In the presence of water, the water-rich side of the sample turned to a very viscous isotropic phase, (Fig. 2d), presumably a cubic phase because it was more viscous than the micellar solution.

Table 2 Thermotropic phase transition temperatures for the dry β-D-xylosides determined by OPM. Error in the measured temperature is ±0.1°C

Lipid	Phase transition and temperature (°C)				
β-Xyl-C_6C_2	Cr	?	L_α	53°C	L_2
β-Xyl-C_8C_4	Cr	?	H_{II}/Col_r[a]	43°C	L_2
β-Xyl-$C_{10}C_6$	Cr	?	H_{II}	51°C	L_2
β-Xyl-$C_{12}C_8$	Cr	?	H_{II}	63°C	L_2
β-Xyl-$C_{14}C_{10}$	Cr	?	H_{II}	56°C	L_2

[a] The SAXS scattering pattern confirmed the birefringent hexagonal texture observed under OPM belongs to a rectangular columnar phase (Col_r)

The third analogue, β-Xyl-$C_{10}C_6$ in an anhydrous state exhibited birefringence but completely changed to an isotropic phase at 51°C. On cooling, it produced the typical fan shape-like texture at 40°C, (Fig. 2e) of a H_{II} phase. This texture remained during water contact penetration experiment at room temperature (Fig. 2f), implying that the phase remains hexagonal (H_{II}). Similarly, β-Xyl-$C_{12}C_8$ gave H_{II} phase both in dry and in the presence of water (Fig. 2g and 2h) except its isotropic phase occurred at a slightly higher temperature of 63°C.

The longest chain member, β-Xyl-$C_{14}C_{10}$ also give H_{II} phase texture in the dry form. However, the texture grew into a viscous isotropic texture during the water contact penetration scan. The viscous isotropic phase was presumed to the cubic phase whose identity shall be confirmed by the small angle scattering experiment.

It is noteworthy that the thermotropic clearing transition temperatures from OPM and of DSC are similar to within the error. In the dry condition, the trend for the clearing transition for the homologous series of the xylosides (see Table 2) is similar to that of the glucosides, but the former have lower clearing temperatures than those of the latter.[19] Moreover, simulation studies of dry glycosides of monosaccharides and disaccharides also agreed qualitatively with the suggestion that the thermotropic clearing transition temperature is related to the number of hydrogen bonds.[25,26] The maltosides with 7OHs have higher clearing transition temperatures compared to the corresponding monosaccharide glucosides with 4OHs. Further comparison between a glucose and a xylose head groups reveals a few degree Celsius difference in clearing temperatures for the shorter chains (-C_6C_2, -C_8C_4 and -$C_{10}C_6$), while the temperature differences in the longer chains (-$C_{12}C_8$ and -$C_{14}C_{10}$) are about two times higher. This observation is also consistent with a previous modelling study of octyl gluco- and galactosides using a density functional theory with the application of atoms in molecules (AIM) analysis. [27] It was shown the glucose head forms an additional hydrogen bond of type HO6---O4 between OH of the hydroxymethyl and oxygen (O4) of the fourth carbon on glucose ring[27]. The presence of this intramolecular hydrogen bond resulted in a higher clearing temperature for the glucoside. In the case of the xyloside, due to the absence of the hydroxymethyl group, this extra intramolecular hydrogen bond could not be formed, hence, compared to the glucoside, less thermal energy is required to drive the xyloside system to the isotropic phase.

3.3 Small angle X-Ray scattering

3.3.1 Thermotropic phases of the xylosides

The scattering pattern of dry β-Xyl-C_6C_2 showed only a single broad peak at q of 0.3042 $Å^{-1}$ at 25°C with d-spacing of 20.4 Å (see Fig. S3 in the Supporting Information). The result confirmed the formation of the L_α phase of β-Xyl-C_6C_2, as observed under an optical polarising microscope.

The broad diffuse peak, corresponding to a spacing of 4.5 Å at a wide angle arises due to the liquid-like disorder of the alkyl chain within the bilayer[28] (see the wide angle spectrum Fig. S3 in the Supporting Information)

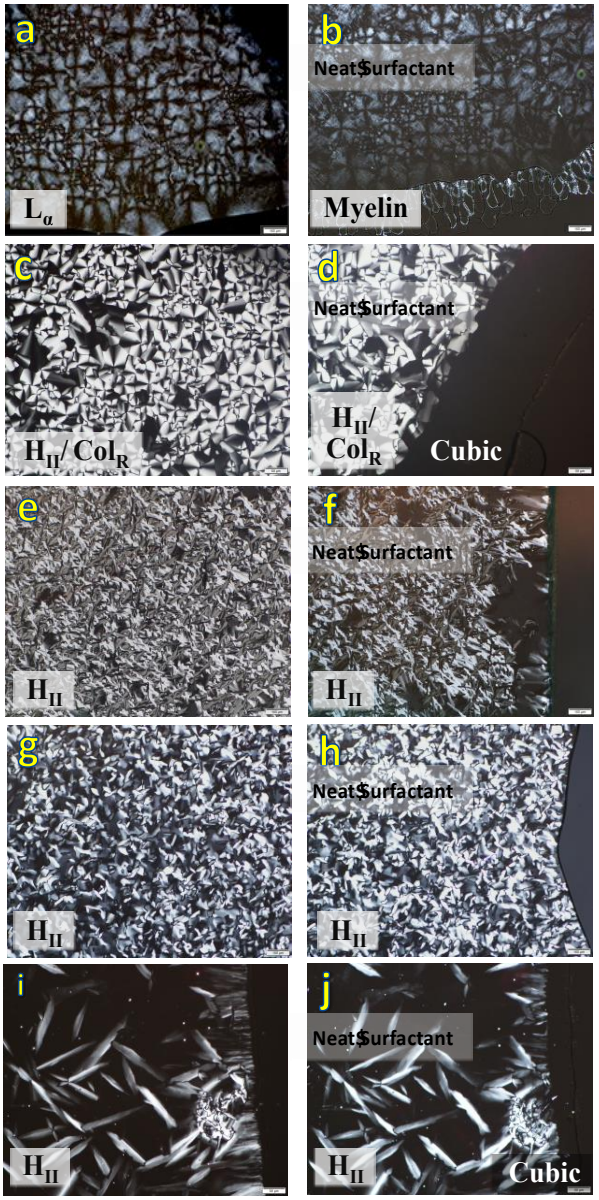

Fig. 2 OPM textures of: (a) L_α of a dry β-Xyl-C_6C_2 (×20); (b) myelin figures from water penetration scan of β-Xyl-C_6C_2 giving hydrated L_α phase after 2 hours (×20); (c) H_{II}/Col_R of dry β-Xyl-C_8C_4 (×10) (d) a growing cubic phase at the water-rich side of the sample after a few hours of water penetration scan (×10); (e) H_{II} of a dry β-Xyl-$C_{10}C_6$ (×10); (f) an H_{II} phase after a water penetration scan of β-Xyl-$C_{10}C_6$ (×10); (g) H_{II} of a dry β-Xyl-$C_{12}C_8$ (×10); (h) an H_{II} phase after a water penetration scan of β-Xyl-$C_{12}C_8$ (×10); (i) H_{II} of a dry β-Xyl-$C_{14}C_{10}$ (×20); (j) a cubic phase after a water penetration scan of β-Xyl-$C_{14}C_{10}$ (×20). All textures were observed at the room temperature.

The SAXS pattern of the dry β-Xyl-C_8C_4 is expected to give characteristic peaks of a H_{II} phase as determined by OPM. However, an uncommon characteristic peaks were obtained which is different from the characteristic Bragg spacing of (1, √3) for the first two reflections in a hexagonal phase (Fig. 3a). Thus, we carefully assigned the Miller indices to determine which crystallographic symmetry the phase belongs to, since these peaks could not be fitted in the SGI software library. The inset in Fig. 3a depicts a linear plot of $1/d^2$ values of the observed peaks versus $(a^2k^2 + b^2h^2)/(a^2b^2)$. The Miller indices (*h,k,l*) are marked as (200), (110), (210), (020), and (220) with the lattice parameters of a = 49.1 Å and b = 25.3 Å. The fitting revealed a rectangular columnar (Col_r) phase (Fig. 3b) which is one of the variants of the hexagonal phase (Fig. 3c), whereby the first order peak (100) in the hexagonal phase splits into (200) and (110) peaks in the Col_r phase (Fig. 3a).[28] Unlike the hexagonal phase (Fig. 3c) which can be modelled as a solid cylinders with hexagonal lattice, the Col_r phase consists of tilted ellipses with respect to the column axis, and the columns are stacked in rectangular 2-D lattices.[29] This produces aggregates that are often called the "ribbon phase". There are several possible arrangements of the columnar phases (see Fig. 3b-f). However, dry β-Xyl-C_8C_4, was identified as the primitive rectangular ribbon phase (*pgg*), because the X-ray characteristic peaks satisfy the restriction that $h+k=2n$ (where n is an integer) for h=0 or k=0. [30] Although the formation of Col_r phase in dry glycolipids is rare, but 4-(4'-*N*,*N*-didodecylaminophenylazo)phenyl 1,2-trans β-D-glucosides[31] has been reported to give a primitive ribbon phase (Col_r) *pmm* (Fig. 3d).

The scattering pattern of dry β-Xyl-$C_{10}C_6$ consists of two peaks with spacing ratios of 1, √4 (Fig. S3 in the Supporting Information). The strong first order peak is observed at q of 0.2595 $Å^{-1}$ and a weaker √4 peak at q = 0.5202 $Å^{-1}$. By comparison with the OPM results, we believe that this arises from a H_{II} phase. Therefore, using 2d/√3 (for a 2-D hexagonal structure), a lattice parameter of 24.2 Å was calculated from the first order peak position. The √3 peak is not seen due to its proximity to the first node in the form factor, whereas the √4 reflection is far enough into the second form factor lobe to be weakly observed. The absence of higher-order peaks √3, √4, √7, etc. has also been found for dry H_{II} phases of Guerbet glucosides[19] and phospholipids.[32] This missing peak is explained by first realising that an observed intensity is the product of both the form factor and the structure. A dry H_{II} phase can be modelled as a 2-D hexagonal lattice of solid cylinders of uniform electron density (consisting of the dry aggregated head groups), together with fluid hydrocarbon chains of uniform electron density. The form factor of a single such cylinder is a Bessel function, whose first node (zero) lies beyond the (10) peak of the hexagonal lattice, but before the next peaks in the pattern. Since the form factor lobes beyond the first node are characteristically of very low amplitude for a solid cylinder, the higher-order peaks are too weak to be observed, and only the (10) peak is seen. In the presence of water (i.e. lyotropic phase), a core of lower electron density relative to the head group is introduced. This effectively makes the Bessel function (form factor) more strongly oscillatory, allowing some of the higher-order peaks to become visible (see Fig. 4c and 4d).[19]

The β-Xyl-$C_{12}C_8$ and β-Xyl-$C_{14}C_{10}$ compounds possess the typical scattering pattern for a H_{II} phase which are the first order peak, and a significantly weak √3 peak giving lattice parameter of 29.2 Å and 31.1 Å respectively (Fig. S3 in the Supporting Information). The SAXS results were consistent with the textures from the OPM studies.

The self-assembly of the dry xylosides implies that the shortest chain lipid with a C_6C_2 branched chain favours lamellar packing whereas the higher members prefer a columnar structure. Meanwhile, the intermediate one ($-C_8C_4$) forms the ribbon phase or Col_r, and the longer chain compounds ($-C_{10}C_6$, $-C_{12}C_8$ and $-C_{14}C_{10}$) give H_{II} structure. The observed results confirm that chain branching supports non-lamellar phases, as reported for other branching systems.[33, 34]

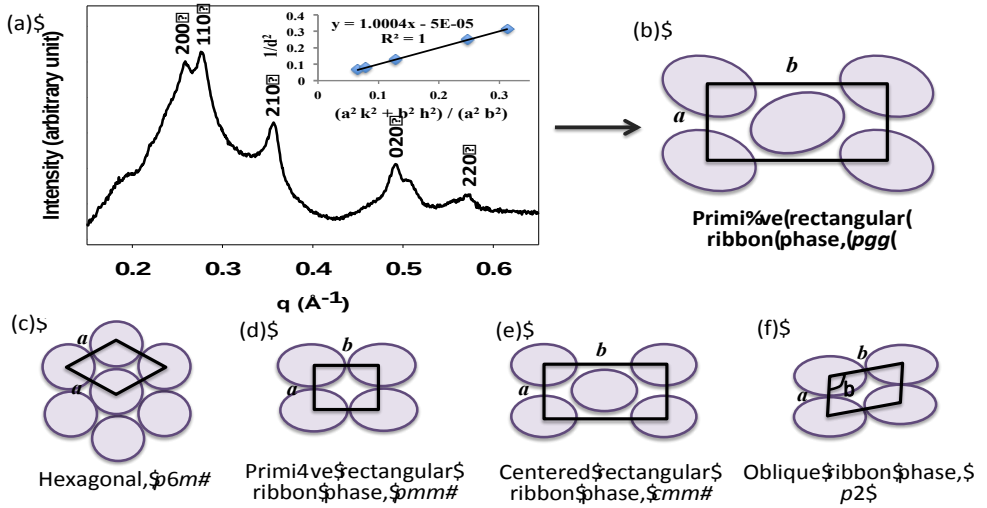

Fig. 3 Small-angle X-ray scattering pattern of (a) dry β-Xyl-C_8C_4 at 25°C. The inset showing a linear fit of a plot of $1/d^{\prime}$ *vs.* $(a^{\prime}k^{\prime} + b^{\prime}h^{\prime})/(a^{\prime}b^{\prime})$ for a Col_r phase; (b-f) possible arrangements of columnar phases. (b) primitive rectangular ribbon phase, *pgg* ; (c) normal hexagonal phase; (d-f) other ribbon phases.

3.3.2 Xylosides in excess water

The Guerbet branched-chain xyloside compounds were studied under excess water at 25°C and prepared at 90% (w/w) water concentration excluding β-Xyl-C_6C_2. It was observed that the lyotropic phases formed by the β-D-xyloside homologous series is related to the average interfacial mean curvature, as is shown in Fig. 4.

The SAXS scattering pattern for β-Xyl-C_6C_2 in excess water was obtained at 50% (w/w). At this concentration, we can clearly detect a two-phase region between a liquid crystal phase and water. This indicates that an excess water point has been attained.

The fully hydrated β-Xyl-C_6C_2 shows an L_α structure with a *d*-spacing of 27.9 Å at 25°C, as shown in Fig. 4a. The lower hydration in L_α phase is a common feature of non-ionic glycolipids such as in single alkyl chain octyl-β-D-glucoside[35] and isoprenoid-chain glycolipids,[14] which implies to stronger intermolecular attractions among sugar head groups in the L_α phase compared to the other phases.

In an excess water condition, β-Xyl-C_8C_4 undergoes a solvation process to form an inverse bicontinuous cubic phase of crystallographic space group *Ia*3*d* (Q_{II}^G). As can be seen from Fig. 4b, Bragg peaks are observed with typical spacing ratios of √6, √8, √14, √16, √20, √22, √24, and √26, with a lattice parameter of 79.2 Å. Of the three Bonnet related structures (Q_{II}^G, Q_{II}^D and Q_{II}^P), a stable Q_{II}^G phase in excess water is rarely observed compared to the other two. This is because the gyroid (G) surface has the most compact space packing with the expectation that it will only exist at lower hydration condition, followed by the diamond (D) and the primitive (P) surfaces. A stable *Ia*3*d* is apparently common for Guerbet glucosides.[17, 19, 36] The asymmetric chain branching is thought to play an important role in stabilising the Q_{II}^G phase in excess water.[17, 37, 38]

Both fully hydrated β-Xyl-$C_{10}C_6$ and β-Xyl-$C_{12}C_8$ were found to give H_{II} phase with strong characteristic peaks of 1, √3, and √4, both with a similar lattice parameter of 35.9 Å (see Fig. 4c, 4d and Table 3) to within the error limit. This result is rather surprising given the dry lattice parameters of the two compounds are quite different.

On increasing the length of the alkyl chain tail, the longest β-Xyl-$C_{14}C_{10}$ compound forms an inverse micellar cubic phase of space group *Fd*3*m* (√8, √11, √16, √19, √24, √27, √32 and √43) in excess water and a lattice parameter of 119.9 Å, as shown in Fig. 4e. The *Fd*3*m* structure consists of two different sizes of spherical inverse micellar aggregates in a cubic lattice packing. The two different sizes of aggregates are non-equivalent with different interfacial mean curvatures.[39]

Unlike the glucoside counterpart (i.e. β-Glc-$C_{14}C_{10}$) which exhibits an H_{II} phase in excess water condition, the corresponding Guerbet xyloside favours the formation of *Fd*3*m* cubic phase. The structural modification involving a replacement of the hydroxylmethyl unit -CH_2-OH group in glucose head group by a proton (in xylose) leads to a smaller, weakly polar head group with a bulky hydrophobic tail. Consequently, the mean interfacial curvature becomes more negative than that of the inverse hexagonal phase. This promotes the formation of inverse spherical aggregates,[39] which is the main feature of *Fd*3*m*.

The *Fd*3*m* phase commonly exists in a ternary system where two lipid components with different amphiphilicities facilitate the formation of inverse micellar aggregates with different diameter.[39] For monoglycerides-based systems, the incorporation of various oils such as hydrocarbon, oleic and elaidic acids into the lipophilic region stabilised the

*Fd*3*m* phase.[40-42] Although the formation of *Fd*3*m* phase in binary system is infrequent, several authors have reported its presence such as in di-alkylxylopyranosyl-glycerol/water[39] and di-phytanylglucosyl-glycerol /water systems.[43]

The xylopyranosyl sugar ring may be able to adopt different conformations in the glycolipid/water binary system. In the xyloside (β-Xyl-$C_{14}C_{10}$)/ water system, these different conformations effectively produce two different hydrophilicities, and lead to the formation of two non-equivalent inverse micellar aggregates, which self-assemble into an *Fd*3*m* phase. The lattice parameters for the self-assembly structures in dry and in excess water are reported in Table 3.

The liquid crystals phases can be differentiated according to their curvature due to the difference of the lateral pressure of the head group region and the hydrocarbon chain region. When the pressure of the head group region is similar to the pressure of the hydrocarbon chain region, the monolayer of the lipids will be flat (lamellar), also known as zero curvature. In contrast, when pressure of head group is larger than the pressure of the hydrocarbon chain region, positive curvature monolayer will formed (normal or direct phase). Negative curvature will form when pressure of head group region is lower (inverse or reverse phase).

The pressure in the hydrocarbon chain region is larger for lipids with longer chains. Comparing the head group and hydrocarbon parts among the five compounds in the solvated state, the lateral pressure in the former remains the same while in the latter depends on the alkyl chain length. The longest chain compound β-Xyl-$C_{14}C_{10}$ gives the *Fd*3*m* phase. This is understandable since the large pressure in the hydrocarbon chain causes the mean curvature to be negative. Both β-Xyl-$C_{12}C_8$ and β-Xyl-$C_{10}C_6$ gives the H_{II} structures with lower pressure in the latter than the former. Interestingly, the curved structure is formed by shorter chain β-Xyl-C_8C_4 with much lower lateral pressure which exhibits an *Ia*3*d* phase. The shortest chain compound β-Xyl-C_6C_2 has zero mean curvature, i.e. its lateral pressure in both head group and hydrocarbon parts is balanced.

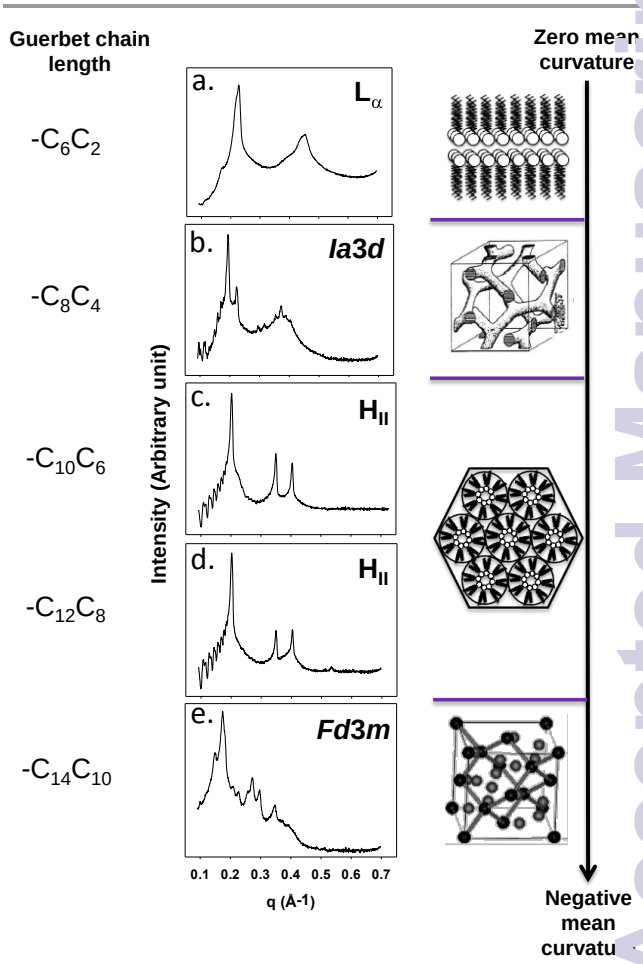

Fig. 4. Small-angle X-ray scattering patterns for Guerbet branched β-D-xylosides in excess water at 25°C.

Table 3 Small-angle X-ray scattering data of the dry and fully hydrated β-D-xylosides at 25°C. Error in lattice parameter measurements is < 0.1 Å.

Lipid	Dry		Fully hydrated	
	Phase	Lattice parameter (Å)	Phase	Lattice parameter (Å)
β-Xyl-C_6C_2	L_α	20.4	L_α	27.9[a]
β-Xyl-C_8C_4	Col_r	a = 49.1, b = 25.3	Q_{II}^G (*Ia*3*d*)	79.2
β-Xyl-$C_{10}C_6$	H_{II}	27.9	H_{II}	35.9
β-Xyl-$C_{12}C_8$	H_{II}	29.2	H_{II}	35.9
β-Xyl-$C_{14}C_{10}$	H_{II}	31.1	I_{II} (*Fd*3*m*)	119.9

[a] The lattice parameter for fully hydrated β-Xyl-C_6C_2 was obtained at 50% (w/w) water concentration. Other samples were prepared at 90% (w/w) water content.

4. Conclusions

Studies on Guerbet xylopyranosides showed rich phase behaviour in their thermotropic and lyotropic states. The shortest -C_6C_2 chain xyloside was found to exhibit L_α phase in both dry and excess water conditions. The neat –C_{8-4} chain compound gave an interesting primitive rectangular ribbon (Col_r) phase of *pgg* symmetry, a rarely reported phase for anhydrous non-ionic glycosides. Meanwhile, the presence of excess water and the asymmetric chain

branching promotes the formation of a stable inverse bicontinuous cubic phase of space group *Ia*3*d* as found for Guerbet glucosides. The H_{II} phase seems to dominate the intermediate ($-C_{10}C_6$) and longer chains β-D-xylosides ($-C_{12}C_8$) in dry and excess water conditions. The dry $-C_{14}C_{10}$ compound exhibited H_{II} phase. When hydrated in excess water, β-Xyl-$C_{14}C_{10}$ forms an inverse micellar cubic phase of space group *Fd*3*m*, an unusual phase for a binary system compared to that of ternary system. This suggests that the xylose sugar head group may be able to adopt different conformations in the two non-equivalent inverse micelles of the *Fd*3*m* cubic phase, which lead to two different effective head group hydrophilicities, and hence behaving more like a ternary system. In general, introduction of chain branching on the hydrocarbon chains gives a relatively large splay to these molecules, which promotes the formation of inverse structures. These include an inverse hexagonal, bicontinuous cubic and micellar cubic phases. Besides that, Guerbet xylosides have lower transition temperatures than the glucoside counterparts due to the presence of merely three hydroxyl groups in a xylose head group. Their ability to form interesting non-lamellar phases at the room temperature makes them ideal candidates for a variety of applications such as controlled release drug-carrier.

Acknowledgements

We thank High Impact Research Grant UM.C/HIR/MOHE/SC/11 from the University of Malaya for the financial support.

References

1. R. Deutschmann and R. F. H. Dekker, *Biotechnol. Adv.*, 2012, **30**, 1627-1640.
2. E. Papadopoulou, A. Hatjiissaak, B. Estrine and S. Marinkovic, *Eur. J. Wood Wood Prod.*, 2011, **69**, 579-585.
3. W. Xu, G. Osei-Prempeh, C. Lema, E. Davis Oldham, R. J. Aguilera, S. Parkin, S. E. Rankin, B. L. Knutson and H.-J. Lehmler, *Carbohydr. Res.*, 2012, **349**, 12-23.
4. M. Ochs, M. Muzard, R. Plantier-Royon, B. Estrine and C. Rémond, *Green Chem.*, 2011, **13**, 2380-2388.
5. B. Ernst, G. W. Hart and P. Sinaÿ, *Carbohydrates in Chemistry and Biology*, Wiley-VCH, Weinheim, 2000.
6. V. Kren and L. Martínková, *Curr. Med. Chem.*, 2001, **8**, 1303-1328.
7. J. W. Goodby, *Liq. Cryst.*, 1998, **24**, 25-38.
8. F. Dumoulin, D. Lafont, P. Boullanger, G. Mackenzie, G. H. Mehl and J. W. Goodby, *J. Am. Chem. Soc.*, 2002, **124**, 13737-13748.
9. C. Van Boeckel and J. Van Boom, *Tetrahedron Lett.*, 1980, **21**, 3705-3708.
10. C. Van Boeckel, P. Westerduin and J. Van Boom, *Tetrahedron Lett.*, 1981, **22**, 2819-2822.
11. J. Israelachvili, *Colloids Surf., A: Physicochemical and Engineering Aspects*, 1994, **91**, 1-8.
12. R. Hashim, A. Sugimura, H. Minamikawa and T. Heidelberg, *Liq. Cryst.*, 2011, **39**, 1-17.
13. H. Nguan, T. Heidelberg, R. Hashim and G. Tiddy, *Liq. Cryst.*, 2010, **37**, 1205-1213.
14. M. Hato, H. Minamikawa, R. A. Salkar and S. Matsutani, *Langmuir*, 2002, **18**, 3425-3429.
15. D. A. Mannock, M. Akiyama, R. N. A. H. Lewis and R. N. McElhaney, *Biochim. Biophys. Acta (BBA) - Biomembranes*, 2000, **1509**, 203-215.
16. H. M. von Minden, M. Morr, G. Milkereit, E. Heinz and V. Vill, *Chem. Phys. Lipids*, 2002, **114**, 55-80.
17. N. I. Zahid, C. E. Conn, N. J. Brooks, N. Ahmad, J. M. Seddon and R. Hashim, *Langmuir*, 2013, **29**, 15794-15804.
18. J. Seddon and R. Templer, *Handbook of Biological Physics*, 1995, **1**, 97-160.
19. N. J. Brooks, H. A. Hamid, R. Hashim, T. Heidelberg, J. M. Seddon, C. E. Conn, S. M. Mirzadeh Husseini, N. I. Zahid and R. S. D. Hussen, *Liq. Cryst.*, 2011, **38**, 1725-1734.
20. P. Claesson, C. Stubenrausch, R. Krustev and I. Johansson, in *Sugar-based surfactants: fundamentals and applications*, ed. C. C. Ruiz, CRC Press, United State of America, 2008, p. 144.
21. J. Barauskas, C. Cervin, F. Tiberg and M. Johnsson, *Phys. Chem. Chem. Phys.*, 2008, **10**, 6483-6485.
22. V. Borshchevskiy, E. Moiseeva, A. Kuklin, G. Büldt, M. Hato and V. Gordeliy, *J. Cryst. Growth*, 2010, **312**, 3326-3330.
23. R. Hashim, H. H. A. Hashim, N. Z. M. Rodzi, R. S. D. Hussen and T. Heidelberg, *Thin Solid Films*, 2006, **509**, 27-35.
24. A. Loewenstein and D. Igner, *Liq. Cryst.*, 1991, **10**, 457-466.
25. S. Ahmadi, V. M. Achari, H. Nguan and R. Hashim, *J. Mol. Model.*, 2014, **20**, 1-12.
26. H. A. Hamid, R. Hashim, J. M. Seddon and N. J. Brooks, in *ICGSCE 2014*, Springer, 2015, pp. 355-362.
27. Z. M. Kotena, R. Behjatmanesh-Ardakani, R. Hashim and V. M. Achari, *J. Mol. Model.*, 2013, **19**, 589-599.
28. S. Chandrasekhar, S. K. Prasad, D. S. Rao and V. Balagurusamy, *PINSA*, 2002, **68**, 175-192.
29. G. C. Shearman, N. J. Brooks, G. J. Tiddy, M. Sztucki, R. H. Templer, R. V. Law, O. Ces and J. M. Seddon, *Soft Matter*, 2011, **7**, 4386-4390.
30. H. Hagslätt, O. Söderman and B. Jönsson, *Liq. Cryst.*, 1992, **12**, 667-688.
31. N. Laurent, D. Lafont, F. Dumoulin, P. Boullanger, G. Mackenzie, P. H. J. Kouwer and J. W. Goodby, *J. Am. Chem. Soc*, 2003, **125**, 15499-15506.
32. J. M. Seddon, *Biochim. Biophys. Acta*, 1990, **1031**, 1-69.
33. D. A. Mannock, M. D. Collins, M. Kreichbaum, P. F. Harper, S. M. Gruner and R. N. McElhaney, *Chem. Phys. Lipids*, 2007, **148**, 26-50.
34. M. Hato, J. Yamashita and M. Shiono, *J. Phys. Chem.*, 2009, **113**, 10196-10209.
35. F. Nilsson, O. Söderman and I. Johansson, *Langmuir*, 1996, **12**, 902-908.
36. M. Salim, N. I. Zahid, C. Y. Liew and R. Hashim, *Liq. Cryst.*, 2015, DOI: 10.1080/02678292.2015.1085104.
37. S. M. Sagnella, C. E. Conn, I. Krodkiewska and C. J. Drummond, *Soft Matter*, 2009, **5**, 4823-4834.

38. T. Kaasgaard and C. J. Drummond, *Phys. Chem. Chem. Phys*, 2006, **8**, 4957-4975.
39. J. M. Seddon, N. Zeb, R. H. Templer, R. N. McElhaney and D. A. Mannock, *Langmuir*, 1996, **12**, 5250-5253.
40. A. Yaghmur, M. Kriechbaum, H. Amenitsch, M. Steinhart, P. Laggner and M. Rappolt, *Langmuir*, 2009, **26**, 1177-1185.
41. A. Yaghmur, B. Sartori and M. Rappolt, *Langmuir*, 2012, **28**, 10105-10119.
42. A. Yaghmur, L. de Campo, S. Salentinig, L. Sagalowicz, M. E. Leser and O. Glatter, *Langmuir*, 2006, **22**, 517-521.
43. H. Minamikawa and M. Hato, *Langmuir*, 1998, **14**, 4503-4509.